Measurement of the neutron F_2 structure function via spectator tagging with CLAS

N. Baillie,[44,16] S. Tkachenko,[33,43] J. Zhang,[33,39] P. Bosted,[39,44] S. Bültmann,[33] M.E. Christy,[16] H. Fenker,[39] K.A. Griffioen,[44] C.E. Keppel,[16] S.E. Kuhn,[33] W. Melnitchouk,[39] V. Tvaskis,[39] K.P. Adhikari,[33] D. Adikaram,[33] M. Aghasyan,[21] M.J. Amaryan,[33] M. Anghinolfi,[22] J. Arrington,[1] H. Avakian,[39] H. Baghdasaryan,[43,33] M. Battaglieri,[22] A.S. Biselli,[11,5] D. Branford,[10] W.J. Briscoe,[15] W.K. Brooks,[41,39] V.D. Burkert,[39] D.S. Carman,[39] A. Celentano,[22] S. Chandavar,[32] G. Charles,[7] P.L. Cole,[18] M. Contalbrigo,[20] V. Crede,[13] A. D'Angelo,[23,36] A. Daniel,[32] N. Dashyan,[45] R. De Vita,[22] E. De Sanctis,[21] A. Deur,[39] B. Dey,[5] C. Djalali,[38] G. Dodge,[33] J. Domingo,[39] D. Doughty,[8,39] R. Dupre,[1] D. Dutta,[31] R. Ent,[39] H. Egiyan,[39,29] A. El Alaoui,[1] L. El Fassi,[1] L. Elouadrhiri,[39] P. Eugenio,[13] G. Fedotov,[38,37] S. Fegan,[42] A. Fradi,[24] M.Y. Gabrielyan,[12] N. Gevorgyan,[45] G.P. Gilfoyle,[35] K.L. Giovanetti,[26] F.X. Girod,[39] W. Gohn,[9] E. Golovatch,[37] R.W. Gothe,[38] L. Graham,[38] B. Guegan,[24] M. Guidal,[24] N. Guler,[33,*] L. Guo,[12,39] K. Hafidi,[1] D. Heddle,[8,39] K. Hicks,[32] M. Holtrop,[29] E. Hungerford,[17] C.E. Hyde,[33] Y. Ilieva,[38,15] D.G. Ireland,[42] M. Ispiryan,[17] E.L. Isupov,[37] S.S. Jawalkar,[44] H.S. Jo,[24] N. Kalantarians,[43] M. Khandaker,[30] P. Khetarpal,[12] A. Kim,[27] W. Kim,[27] P.M. King,[19,32] A. Klein,[33] F.J. Klein,[6] A. Klimenko,[33] V. Kubarovsky,[39,34] S.V. Kuleshov,[41,25] N.D. Kvaltine,[43] K. Livingston,[42] H.Y. Lu,[5,38] I .J .D. MacGregor,[42] Y. Mao,[38] N. Markov,[9] B. McKinnon,[42] T. Mineeva,[9] B. Morrison,[2] H. Moutarde,[7] E. Munevar,[15] P. Nadel-Turonski,[39,15] A. Ni,[27] S. Niccolai,[24] I. Niculescu,[26] G. Niculescu,[26] M. Osipenko,[22] A.I. Ostrovidov,[13] L. Pappalardo,[20] K. Park,[39,27] S. Park,[13] E. Pasyuk,[39,2] S. Anefalos Pereira,[21] S. Pisano,[21,24] S. Pozdniakov,[25] J.W. Price,[3] S. Procureur,[7] Y. Prok,[8,43] D. Protopopescu,[42] B.A. Raue,[12,39] G. Ricco,[22,14] D. Rimal,[12] M. Ripani,[22] G. Rosner,[10] P. Rossi,[21] F. Sabatié,[7] M.S. Saini,[13] C. Salgado,[30] D. Schott,[12] R.A. Schumacher,[5] E. Seder,[9] Y.G. Sharabian,[39] D.I. Sober,[6] D. Sokhan,[24] S. Stepanyan,[39] S.S. Stepanyan,[27] P. Stoler,[34] S. Strauch,[38] M. Taiuti,[14] W. Tang,[32] M. Ungaro,[9] M.F. Vineyard,[40] E. Voutier,[28] D.P. Watts,[10] L.B. Weinstein,[33] D.P. Weygand,[39] M.H. Wood,[4,38] L. Zana,[29] and B. Zhao[44,9]

(The CLAS Collaboration)

[1] *Argonne National Laboratory, Argonne, Illinois 60439*
[2] *Arizona State University, Tempe, Arizona 85287*
[3] *California State University, Dominguez Hills, Carson, California 90747*
[4] *Canisius College, Buffalo, New York 14208*
[5] *Carnegie Mellon University, Pittsburgh, Pennsylvania 15213*
[6] *Catholic University of America, Washington, DC 20064*
[7] *CEA, Centre de Saclay, Irfu/Service de Physique Nucléaire, 91191 Gif-sur-Yvette, France*
[8] *Christopher Newport University, Newport News, Virginia 23606*
[9] *University of Connecticut, Storrs, Connecticut 06269*
[10] *Edinburgh University, Edinburgh EH9 3JZ, United Kingdom*
[11] *Fairfield University, Fairfield, Connecticut 06824*
[12] *Florida International University, Miami, Florida 33199*
[13] *Florida State University, Tallahassee, Florida 32306*
[14] *Università di Genova, 16146 Genova, Italy*
[15] *The George Washington University, Washington, DC 20052*
[16] *Hampton University, Hampton, Virginia 23668*
[17] *University of Houston, Houston, Texas 77204*
[18] *Idaho State University, Pocatello, Idaho 83209*
[19] *University of Illinois at Urbana-Champaign, Urbana, Illinois 61801*
[20] *INFN, Sezione di Ferrara, 44100 Ferrara, Italy*
[21] *INFN, Laboratori Nazionali di Frascati, 00044 Frascati, Italy*
[22] *INFN, Sezione di Genova, 16146 Genova, Italy*
[23] *INFN, Sezione di Roma Tor Vergata, 00133 Rome, Italy*
[24] *Institut de Physique Nucléaire ORSAY, Orsay, France*
[25] *Institute of Theoretical and Experimental Physics, Moscow, 117259, Russia*
[26] *James Madison University, Harrisonburg, Virginia 22807*
[27] *Kyungpook National University, Daegu 702-701, Republic of Korea*
[28] *LPSC, Universite Joseph Fourier, CNRS/IN2P3, INPG, Grenoble, France*
[29] *University of New Hampshire, Durham, New Hampshire 03824*
[30] *Norfolk State University, Norfolk, Virginia 23504*
[31] *Mississippi State University, Mississippi State, Mississippi 39762*
[32] *Ohio University, Athens, Ohio 45701*
[33] *Old Dominion University, Norfolk, Virginia 23529*
[34] *Rensselaer Polytechnic Institute, Troy, New York 12180*
[35] *University of Richmond, Richmond, Virginia 23173*

[36] Universita' di Roma Tor Vergata, 00133 Rome, Italy
[37] Skobeltsyn Nuclear Physics Institute, Skobeltsyn Nuclear Physics Institute, 119899 Moscow, Russia
[38] University of South Carolina, Columbia, South Carolina 29208
[39] Thomas Jefferson National Accelerator Facility, Newport News, Virginia 23606
[40] Union College, Schenectady, New York 12308
[41] Universidad Técnica Federico Santa María, Casilla 110-V Valparaíso, Chile
[42] University of Glasgow, Glasgow G12 8QQ, United Kingdom
[43] University of Virginia, Charlottesville, Virginia 22901
[44] College of William and Mary, Williamsburg, Virginia 23187
[45] Yerevan Physics Institute, 375036 Yerevan, Armenia
(Dated: December 8, 2011)

We report on the first measurement of the F_2 structure function of the neutron from semi-inclusive scattering of electrons from deuterium, with low-momentum protons detected in the backward hemisphere. Restricting the momentum of the spectator protons to $\lesssim 100$ MeV/c and their angles to $\gtrsim 100^\circ$ relative to the momentum transfer allows an interpretation of the process in terms of scattering from nearly on-shell neutrons. The F_2^n data collected cover the nucleon-resonance and deep-inelastic regions over a wide range of Bjorken x for $0.65 < Q^2 < 4.52$ GeV^2, with uncertainties from nuclear corrections estimated to be less than a few percent. These measurements provide the first determination of the neutron to proton structure function ratio F_2^n/F_2^p at $0.2 \lesssim x \lesssim 0.8$, essentially free of nuclear corrections.

PACS numbers: 13.60-r, 13.60.Hb, 14.20.Dh

Structure functions of the nucleon reflect the defining features of QCD: asymptotic freedom at short distances and quark confinement at long distance scales. After four decades of deep-inelastic lepton scattering (DIS) measurements at facilities worldwide, an impressive quantity of data has been collected, extending over several orders of magnitude in Bjorken x (the fraction of the nucleon's momentum carried by the struck quark) and Q^2 (the squared 4-momentum transfer). These data have provided strong constraints on the quark and gluon (or parton) momentum distribution functions (PDFs) of the nucleon.

Although the structure of the proton has been well determined, the absence of high density, free neutron targets has meant that neutron structure functions must be inferred from experiments on nuclear targets, particularly deuterium. In regions of kinematics where most of the momentum resides with a single quark, $x \gtrsim 0.5$, uncertainties in the nuclear corrections in deuterium result in large uncertainties in the extracted neutron structure functions [1–6].

Determining structure functions and PDFs at large x is important for several reasons. For example, one of the long-standing puzzles in hadronic physics is the behavior of the ratio of d to u quark PDFs in the proton in the limit $x \to 1$ [2]. A number of predictions have been made for the d/u ratio in this limit, from perturbative and nonperturbative QCD arguments [7], but because of the lack of neutron data these have never been verified.

A better knowledge of neutron structure functions in the resonance region is also needed to help unravel the full isospin structure of the resonant and nonresonant contributions to the cross section, as well as to provide critical input for interpreting inclusive polarization asymmetry measurements. An important question in the resonance region is whether Bloom-Gilman duality holds as well for the neutron as it does for the proton [8, 9]. Furthermore, model-independent determinations of F_2 are essential for evaluating the efficacy of model-dependent extractions [10] of F_2^n in the resonance region from inclusive deuterium data.

It has been suggested [11–13] that one can greatly reduce the nuclear model uncertainties associated with scattering on the deuteron by selecting events with low momentum protons produced at backward kinematics relative to the momentum transfer. Tagging backward-moving spectator protons minimizes final-state interactions (FSIs) [14, 15], and the restriction to low momenta ensures that the scattering takes place on a nearly on-shell neutron. Furthermore, by measuring the momentum of the recoiling proton, one can correct for the initial motion of the struck neutron, all but eliminating Fermi smearing effects.

In this Letter we report on the first direct extraction of the neutron F_2^n structure function by tagging spectator protons in semi-inclusive electron scattering from the deuteron. In the impulse approximation, where the virtual photon scatters incoherently from a single nucleon, the differential cross section for the reaction $d(e,e'p_s)X$ is given by [12, 15]

$$\frac{d\sigma}{dx dQ^2 d^3p_s/E_s} = \frac{2\alpha^2}{xQ^4}\left(1 - y - \frac{x^2y^2M^2}{Q^2}\right) \times \left(\mathcal{F}_2^d + 2\tan^2\frac{\theta}{2}\,\frac{\nu}{M}\mathcal{F}_1^d\right), \quad (1)$$

where α is the fine structure constant, $p_s = |\boldsymbol{p}_s|$ and

*Current address: Los Alamos National Laborotory, Los Alamos, New Mexico 87544

$E_s = \sqrt{M^2 + \boldsymbol{p}_s^2}$ are the spectator nucleon momentum and energy in the laboratory frame, and M is the nucleon mass. Here $x = Q^2/2M\nu$ is the Bjorken scaling variable, with ν the energy transfer to the deuteron, and $Q^2 = -q^2$ is the square of the exchanged virtual photon four-momentum vector q. The variable $y = \nu/E$ is the fraction of the incident electron energy E transferred, and θ is the electron scattering angle. Additional structure functions that vanish after integration over the azimuthal angle of the spectator have been omitted in Eq. (1).

The semi-inclusive deuteron structure functions $\mathcal{F}^d_{1,2}$ are in general functions of four variables, $\mathcal{F}^d_{1,2} = \mathcal{F}^d_{1,2}(x, Q^2, \alpha_s, p_s^\perp)$, where $\alpha_s = (E_s - p_s^z)/M$ is the fraction of the deuteron's light-cone momentum carried by the spectator proton, and p_s^z and $p_s^\perp$ are its longitudinal and transverse momenta, respectively. In the impulse approximation the functions $\mathcal{F}^d_{1,2}$ are related to the (effective) neutron structure functions $F^n_{1,2}$ and the deuteron spectral function $S(\alpha_s, p_s^\perp)$; in the limit of large Q^2 and small $p_s^\perp/M$ one has [12]

$$\mathcal{F}^d_{1,2} \propto S(\alpha_s, p_s^\perp)\, F^n_{1,2}(x^*, Q^2, p^2), \qquad (2)$$

where $x^* = Q^2/2p\cdot q \approx x/(2-\alpha_s)$ is the Bjorken scaling variable of the struck neutron in the deuteron, and $p^2 = (M_d - E_s)^2 - \boldsymbol{p}_s^2$ is its virtuality, with M_d the deuteron mass. The spectral function is proportional to the square of the deuteron wave function. In terms of x^* the inferred invariant mass squared of the struck neutron remnant is given by $W^{*2} = (p+q)^2 = p^2 + Q^2(1-x^*)/x^*$, in contrast to the usual definition of $W^2 = M^2 + Q^2(1-x)/x$ for a free nucleon.

For inclusive scattering on the deuteron one integrates Eq. (1) over all spectator momenta p_s and expresses the extracted structure function in terms of the variables x or W; for the tagged reaction the detection of a proton at specific kinematics selects a fixed x^* and W^*. Moreover, the restriction to backward-moving protons serves to minimize the probability of the recoil proton rescattering with the debris of the struck neutron. Calculations within hadronization models suggest [14, 15] that for spectator momenta below ~ 100 MeV/c final-state interaction effects distort the spectral function by $\lesssim 5\%$, provided spectator angles θ_{pq} are above 100°. Backward kinematics also suppresses contributions from low momentum protons emanating from the hadronic debris of the struck neutron, which distort the spectral function at the $\lesssim 1\%$ level [13]. These theoretical calculations are corroborated by both existing data [16] and by our own analysis of the full data set [17].

Because the neutron is bound inside the deuterium nucleus with binding energy $\varepsilon_d = -2.2$ MeV, it can never be exactly on-shell since $p^2 - M^2 \approx 2M\varepsilon_d - 2\boldsymbol{p}_s^2 < 0$, even when it is at rest. The dependence on the neutron's virtuality may introduce additional differences between the effective neutron structure functions in Eq. (2) and their on-shell values. However, since the bound neutron is ≈ 13 MeV away from its mass-shell for $p_s = 100$ MeV/c (and only 7.5 MeV for $p_s = 70$ MeV/c) the uncertainty introduced in extrapolating to the on-shell point is minimal. Indeed, quantitative estimates of the off-shell dependence of the neutron structure functions in relativistic quark-spectator diquark models [18, 19] and models that consider the effects of evaluating the structure function at a shifted energy transfer [20] give corrections to the on-shell structure functions of $\lesssim 1\%$ for $p_s < 100$ MeV/c.

The BoNuS (Barely off-shell Nucleon Structure) experiment ran in 2005 using the CEBAF Large Acceptance Spectrometer (CLAS) [21] in Hall B at Jefferson Lab. Electrons scattered from a thin deuterium gas target were detected by CLAS and the spectator protons were measured with the BoNuS Radial Time Projection Chamber (RTPC) [22]. Production data were taken at three beam energies, 2.140, 4.223 and 5.262 GeV, with an additional set of calibration data taken at 1.099 GeV. The kinematic coverage includes final-state invariant masses from the quasi-elastic peak up to $W^* \approx 3$ GeV, and momentum transfers Q^2 from 0.2 GeV^2 to ≈ 5.0 GeV^2.

The RTPC reconstructed the three-dimensional tracks of spectator protons in a 3 cm wide annular ionization volume, using gaseous electron multipliers (GEMs) to amplify the ionization electrons. The signals were read out via a grid of conducting pads on a cylindrical outer surface in 114 ns increments of time, yielding up to 60 points in radius, azimuth and z (the distance along the beam direction) for each track. The 170 mm long target inside the 200 mm long RTPC allowed detection of spectator protons with polar angles $20° < \theta_s < 160°$ in the lab frame, covering 295° in azimuth. This provides good spectator acceptance over the range $-0.9 < \cos\theta_{pq} < 0.9$. The detector was immersed in a 4 T solenoidal magnetic field which suppressed electromagnetic background (Møller electrons) and bent the proton tracks. Measuring the curvature allowed reconstruction of the proton momentum, and measuring the total ionization charge associated with a track enabled the separation of protons from other hadrons through their specific energy loss. By requiring tracks to be in time with the detected electron (within 2 μs) and to trace back to the electron vertex in z (within 30 mm), accidental backgrounds could be suppressed to about 20%. Using events with a larger distance in z between the electron and proton vertices as a sample of accidentals, this background was subtracted from the data. Details of the RTPC construction and performance are found in Ref. [22].

The data were also corrected for pions misidentified as electrons in CLAS and for electrons coming from pair-symmetric decays of mesons and photons. Cuts on $y \leq 0.8$ eliminated events with large radiative corrections. Lower limits were placed on x for each bin in Q^2 to remove acceptance edge effects. The low density of material in the path of the outgoing protons allowed them to be identified with momenta down to 70 MeV/c. The analysis was restricted to protons with momenta less than 100 MeV/c, and angles relative to the momentum transfer vector $\boldsymbol{q}$ of more than 100° – in the following

referred to as the kinematic bin $\Delta^{(\mathrm{VIP})}\boldsymbol{p}_s$ for "very important protons" (VIPs).

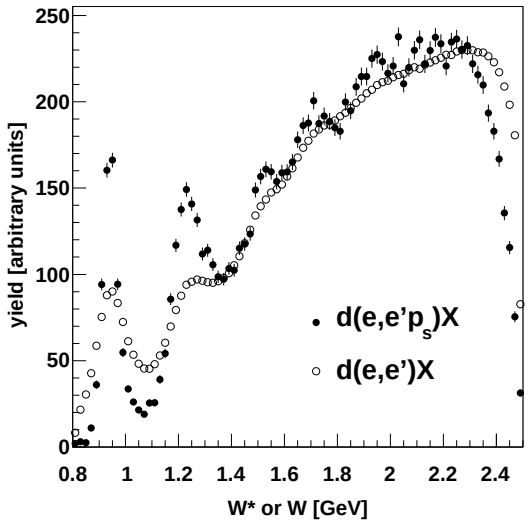

FIG. 1: Yield for the semi-inclusive $d(e,e'p_s)X$ reaction with a backward-moving spectator proton as a function of the invariant mass W^* of the neutron debris, compared with the yield for the inclusive $d(e,e')X$ reaction as a function of the customary kinematic variable W. Yields integrated over W and W^* are normalized to be the same. The data are for the 4.223 GeV beam energy and are averaged over the acceptance of CLAS. For backward-moving spectators $W^* < W$, which explains the leftward shift of the high W^* cutoff in the semi-inclusive spectrum with respect to the inclusive case.

The utility of the spectator tagging method is illustrated in Fig. 1, where a typical semi-inclusive yield for the $d(e,e'p_s)X$ reaction is shown as a function of the invariant mass W^* of the neutron's hadronic debris, and the corresponding inclusive yield for the $d(e,e')X$ reaction is shown as a function of the usual invariant mass W for a neutron struck at rest in the lab frame. The quasi-elastic and $\Delta(1232)$ resonance peaks are largely smeared out by the nuclear Fermi motion in the inclusive spectrum, whereas the neutron elastic and resonance peaks clearly stand out in the semi-inclusive spectrum. The elastic neutron peak for $d(e,e'p_s)X$ has a Gaussian width of 31 MeV, which is only 20% larger than that for a proton target measured with CLAS.

For our final results, we formed the ratio R_{exp} of the acceptance-corrected yields for $d(e,e'p_s)X$ in the individual W^* (or x^*) and Q^2 bins for a spectator proton within the bin $\Delta^{(\mathrm{VIP})}\boldsymbol{p}_s$, divided by the similarly corrected yield measured for $d(e,e')X$ at the corresponding W or x,

$$R_{\mathrm{exp}} = \frac{N_{\mathrm{tagged}}(\Delta Q^2, \Delta W^*, \Delta^{(\mathrm{VIP})}\boldsymbol{p}_s)/\mathcal{A}_e(Q^2, W^*)}{N_{\mathrm{incl}}(\Delta Q^2, \Delta W)/\mathcal{A}_e(Q^2, W)}. \tag{3}$$

In this ratio, the total luminosity of the experiment cancels, and the corrections due to the CLAS acceptance for the scattered electrons, $\mathcal{A}_e$, largely cancel, as this enters the numerator and denominator at rather similar kinematics. The acceptance $\mathcal{A}_e$ was determined from the ratio of inclusive electron count rates and the known ed cross section [24]. Although $\mathcal{A}_e$ varied by a factor of 2, the corrections to the ratio were less than 10%. Radiative corrections were applied to both numerator and denominator based on the prescription by Mo and Tsai [23], using models [24] of F_2^n, F_2^d and the ratio of longitudinal to transverse cross sections as input for the calculations. These also canceled to a large extent in the ratio and were less than 10%.

In the spectator approximation of Eq. (2), the ratio R_{exp} is directly proportional to the ratio of (free) structure functions F_2^n/F_2^d multiplied by the spectral function $S(\alpha_s, p_s^\perp)$ integrated over the proton acceptance $\mathcal{A}_p$ of the RTPC within the VIP cuts,

$$R_{\mathrm{exp}} = \frac{F_2^n(W^*, Q^2)}{F_2^d(W, Q^2)} \int_{\mathrm{VIP}} d\alpha_s dp_s^\perp \, \mathcal{A}_p(\alpha_s, p_s^\perp)\, S(\alpha_s, p_s^\perp). \tag{4}$$

The integral I_{VIP} in Eq. (4) is largely independent of kinematics, and $(F_2^n/F_2^p)_{\mathrm{exp}} = R_{\mathrm{exp}}(F_2^d/F_2^p)/I_{\mathrm{VIP}}$, in which F_2^d and F_2^p are well-measured values parameterized in Ref. [24]. The normalization constant I_{VIP} was chosen for the whole data set using $F_2^n/F_2^p = 0.695$ at $x = 0.3$, where nuclear effects are small, with an uncertainty of 3% from the CJ global PDF fits [5]. The rms variation in the normalization constant I_{VIP} for subsets in W^* and Q^2 was 3.4%, which was included in the systematic error. The structure function $(F_2^n)_{\mathrm{exp}}$ was obtained by multiplying $(F_2^n/F_2^p)_{\mathrm{exp}}$ by the values of F_2^p parameterized in Ref. [24]. The final systematic errors include uncertainties on F_2^d and F_2^p and possible deviations from the (implicit) assumption that the longitudinal to transverse cross section ratios are the same for d, p and n, as well as residual background, acceptance and radiative correction uncertainties. A conservative systematic error of 3% was assigned to possible violations of the spectator assumptions due to final-state interactions and off-shell effects [12–15]. An additional 3% (rms) uncertainty arises from the global fit for F_2^d.

A representative sample of the neutron F_2^n spectra is shown in Fig. 2, compared with a phenomenological parametrization of F_2^n [24] obtained from inclusive F_2^d and F_2^p data using a model of nuclear effects, and an extraction [10] of F_2^n from recent F_2^d and F_2^p data using the nuclear smearing corrections of Ref. [25]. (The complete spectra for all kinematics are published in the CLAS database [26].)

The comparison shows reasonable overall agreement between the BoNuS data and the model-dependent F_2^n extractions [10, 24] from inclusive data, but highlights some residual discrepancies. In particular, at the lowest Q^2 values both the parametrization [24] and the model-dependent extraction [10] underestimate the F_2^n data, especially in the vicinity of the $\Delta(1232)$ peak. At larger Q^2 the models are in better agreement with the data in the Δ region, but overestimate it somewhat in the third res-

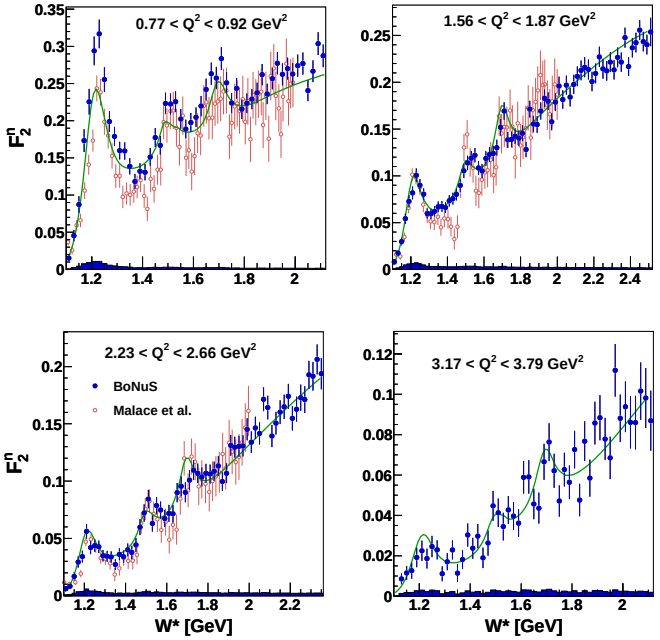

FIG. 2: (Color online) Typical F_2^n spectra from the BoNuS experiment (filled circles) as a function of W^* for the various Q^2 indicated. For comparison the model-dependent extraction from inclusive F_2^d data (open circles) [10] and the phenomenological model from Ref. [24] (solid curve) are also shown. The error bars on the data points are statistical, and the band along the abscissa represents the systematic error without the overall 3% normalization uncertainty or the 3% spectator approximation uncertainty.

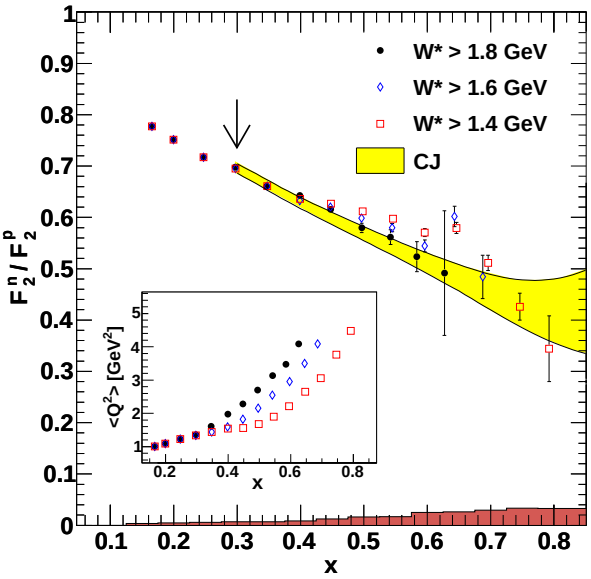

FIG. 3: (Color online) Ratio F_2^n/F_2^p versus x for various lower limits on W^*. The error bars are statistical, with the total (correlated and uncorrelated) systematic uncertainties indicated by the band along the abscissa. This band does not include the overall 3% normalization uncertainty or the 3% spectator approximation uncertainty. The data are compared with the recent parametrization from the CJ global analysis [5], with the upper and lower uncertainty limits indicated by the solid lines. The inset shows the average Q^2 as a function of x for each W^* cut. For these data α_s is in the range 1.0-1.2. The arrow indicates the point at which the data are normalized to the CJ value. A single normalization constant $I_{\rm VIP}$ was used for all data.

onance region at $Q^2 \sim 2.5$ GeV^2. This suggests that either the nonresonant neutron contribution assumed in the model [24], or possibly the treatment of nuclear corrections in deuterium, need to be reconsidered.

The ratio of neutron to proton structure functions, F_2^n/F_2^p, is shown in Fig. 3 as a function of x for various W^* cuts ($W^* > 1.4$, 1.6 and 1.8 GeV), and compared with the ratio from the recent CJ global PDF fit [5] at matching kinematics. The range for the global fit arises from experimental and PDF fit uncertainties, as well as from uncertainties in the treatment of nuclear corrections in the analysis of inclusive F_2^d data, which increase dramatically at high x [2, 5]. Where the kinematics overlap, the data for the $W^* > 1.8$ GeV cut are in good agreement with the global PDF fit for $0.3 \lesssim x \lesssim 0.6$ (the data at the lowest x values are outside of the range of validity of the global fit, which is restricted to $Q^2 > 1.69$ GeV^2). Note that a bump in F_2^n/F_2^p appears near $x^* = 0.65$ when relaxing the W^* cut from 1.8 GeV to 1.6 or 1.4 GeV, which likely indicates that a resonance in this region is significantly enhanced in the neutron relative to the inelastic F_2^n/F_2^p background.

In summary, we have presented results on the first measurement of the neutron F_2^n structure function using the spectator tagging technique, where selection of low-momentum protons at backward angles ensures scattering from a nearly on-shell neutron in the deuteron. We identify well-defined neutron resonance spectra in each of the three prominent nucleon resonance regions, which broadly agree with earlier model-dependent extractions from inclusive deuteron and proton data, but with systematic discrepancies above the second resonance region. The new, high-precision data will be useful in constraining models and parametrizations of neutron structure in the resonance region and beyond, and allow direct tests of quark-hadron duality in the neutron [9, 10]. These will be the subjects of future publications.

When combined with previous F_2^d/F_2^p measurements, the new F_2^n/F_2^d BoNuS data are used to reconstruct the ratio of neutron to proton F_2^n/F_2^p structure functions up to $x \approx 0.6$ in DIS kinematics, and up to $x \approx 0.8$ in the resonance region, essentially free of nuclear corrections. The results for the more stringent $W^* > 1.8$ GeV cuts agree well with the shape of recent global PDF fits [4, 5] in regions where the kinematics overlap, $0.3 \lesssim x \lesssim 0.6$, but show clear resonant structure at large x for lower-W^* cuts. The precision of the new data, particularly in the DIS region, will be important in reducing uncertainties in

global PDF analyses [4, 5], and extensions of the BoNuS experiment with the future 12 GeV Jefferson Lab will provide even stronger constraints on PDFs up to $x \approx 0.8$ [27].

Acknowledgments

We thank the staff of the Jefferson Lab accelerator and Hall B for their support on this experiment. This work was supported by DOE contract No. DE-AC05-06OR23177, under which Jefferson Science Associates, LLC operates Jefferson Lab, and by the Chilean Comisión Nacional de Investigación Científica y Tecnológica (CONICYT), the Italian Istituto Nazionale di Fisica Nucleare, the French Centre National de la Recherche Scientifique, the French Commissariat à l'Energie Atomique, the U.S. Department of Energy, the National Science Foundation, the UK Science and Technology Facilities Council (STFC), the Scottish Universities Physics Alliance (SUPA), and the National Research Foundation of Korea.

[1] L. Whitlow *et al.*, Phys. Lett. B **282**, 475 (1992).
[2] W. Melnitchouk and A. W. Thomas, Phys. Lett. B **377**, 11 (1996).
[3] J. Arrington *et al.*, J. Phys. G **36**, 025005 (2009).
[4] A. Accardi *et al.*, Phys. Rev. D **81**, 034016 (2010).
[5] A. Accardi *et al.*, Phys. Rev. D **84**, 014008 (2011).
[6] R. J. Holt and C. D. Roberts, Rev. Mod. Phys. **82**, 2991 (2010).
[7] R. P. Feynman, *Photon-Hadron Interactions*, Benjamin, Reading, Massachusetts, 1972; F. E. Close, Phys. Lett. **43** B, 422 (1973); G. R. Farrar and D. R. Jackson, Phys. Rev. Lett. **35**, 1416 (1975).
[8] E. D. Bloom and F. J. Gilman, Phys. Rev. Lett. **25**, 1140 (1970).
[9] W. Melnitchouk, R. Ent and C. Keppel, Phys. Rep. **406**, 127 (2005).
[10] S. P. Malace, Y. Kahn, W. Melnitchouk and C. E. Keppel, Phys. Rev. Lett. **104**, 102001 (2010); S. P. Malace, private communication.
[11] L. Frankfurt and M. Strikman, Phys. Rep. **160**, 235 (1988).
[12] W. Melnitchouk, M. Sargsian and M. Strikman, Z. Phys. A **359**, 99 (1997); M. Sargsian and M. Strikman, Phys. Lett. B **639**, 223 (2006).
[13] S. Simula, Phys. Lett. B **387**, 245 (1996).
[14] C. Ciofi degli Atti, L. P. Kaptari and B. Z. Kopeliovich, Eur. Phys. J. A **19**, 133 (2004).
[15] W. Cosyn and M. Sargsian, Phys. Rev. C **84**, 014601 (2011).
[16] A. V. Klimenko *et al.*, Phys. Rev. C **73**, 035212 (2006).
[17] S. Tkachenko *et al.*, in preparation.
[18] W. Melnitchouk, A. W. Schreiber and A. W. Thomas, Phys. Rev. D **49**, 1183 (1994); Phys. Lett. B **335**, 11 (1994).
[19] F. Gross and S. Liuti, Phys. Rev. C **45**, 1374 (1992).
[20] L. Heller and A. W. Thomas, Phys. Rev. C **41**, 2756 (1990).
[21] B. A. Mecking *et al.*, Nucl. Instrum. Meth. **A503**, 513 (2003).
[22] H. Fenker *et al.*, Nucl. Instrum. Meth. A **592**, 273 (2008).
[23] L. Mo and Y. Tsai, Rev. Mod. Phys. **41**, 205 (1969).
[24] P. E. Bosted and M. E. Christy, Phys. Rev. C **77**, 065206 (2008); M. E. Christy and P. E. Bosted, Phys. Rev. C **81**, 055213 (2010).
[25] S. Kulagin and R. Petti, Nucl. Phys. **A765**, 126 (2006); Y. Kahn, W. Melnitchouk and S. A. Kulagin, Phys. Rev. C **79**, 035205 (2009).
[26] CLAS Experimental Database, http://clasweb.jlab.org/physicsdb/.
[27] *The Structure of the Free Neutron at Large x-Bjorken*, Jefferson Lab experiment E12-06-113, S. Bültmann *et al.*, co-spokespersons.